

Palladium(II)-Assisted Copolymerization of Ethylene and CO: Influence of the Chain End on the Regularity of the Polymer

Peter Margl[†] and Tom Ziegler^{*‡}

Department of Chemistry, University of Calgary, 2500 University Drive N.W.,
Calgary, Alberta, Canada T2N 1N4

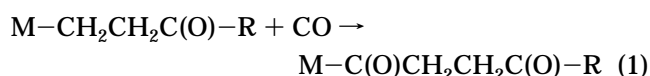
Received June 28, 1996[®]

A theoretical study based on nonlocal density functional theory has been carried out on the Pd(II)-assisted homogeneous catalytic copolymerization of olefin and carbon monoxide, where the catalytic center is modeled by Pd(II) coordinated to $\text{PH}_2\text{CH}=\text{CHPH}_2$ and the olefin is modeled by C_2H_4 . The investigation concentrated on the energetics of the chain propagation mechanism in the presence of a copolymer chain end with a carbonyl group coordinated to the metal center. With CO misinsertion ruled out in a previous work,¹ the present investigation rules out ethylene misinsertion into a growing polyketone chain due to the lack of a thermodynamically stable ethylene π -complex and the high barrier (+78 kJ/mol) associated with insertion of ethylene into the Pd– $\text{C}_2\text{H}_4\text{COR}$ bond. On the other hand, insertion of CO into a Pd– $\text{C}_2\text{H}_4\text{COR}$ bond is favored by a rather stable CO precursor complex (–32 kJ/mol) and by a low activation barrier (+49 kJ/mol).

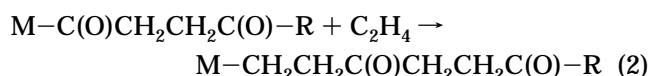
Introduction

Olefin-CO copolymers (polyketones) are considered to be of great technical importance^{2–9} due to their mechanical strength and ability to photodegrade. The carbonyl groups can be efficiently modified further, thus allowing for the introduction of new functionalities into the polymer. Due to recent advances in the synthesis of olefin-CO copolymers, it is now possible to synthesize chiral copolymers with the use of Pd(II)-based homogeneous catalysts, such as those proposed by Jiang and Sen³ where the chiral copolymer is built up from prochiral constituents.

Copolymerization of an olefin with carbon monoxide involves the insertion of CO into a metal-alkyl bond



alternating with the insertion of an olefin into the metal-acyl bond



Many of the aspects connected to CO/olefin copolymerization^{2,10} have been investigated experimentally. We

have more recently added to the body of knowledge by a theoretical study based on density functional theory (DFT).¹ Both experimental results and theory^{1,2,10} point to the premise that CO/olefin copolymerization is thermodynamically less favorable than pure olefin polymerization. However, copolymerization still takes place because CO insertion in eq 1 has a much lower activation barrier than the corresponding olefin insertion into a metal-alkyl bond. An alternative pure CO polymerization on the other hand is not possible since olefin insertion into the metal-acyl bond in eq 2 is favored both kinetically and thermodynamically over CO insertion.

Our previous DFT study¹ investigated in detail the generic aspects of the copolymerization process, neglecting the fact that the polyketone chain might modify the insertion barriers by forming chelating bonds with the metal center. We shall consider this point here by modeling the two processes in eqs 1 and 2 with a growing chain sufficiently long to allow for chelation (Figure 1). The same growing chain will be used to further study the alternative "misinsertion" of an olefin into the metal-alkyl bond (Figure 2). After the completion of our calculations, Rix et al.¹⁰ published accurate experimental energetics for some of the elementary reaction steps involved in CO/ C_2H_4 copolymerization, affording a rare opportunity for a validation of the DFT approach in studies of organometallic reactions. In this work we shall compare the energetics derived by this and a previous study¹ to the experimentally obtained values of Rix et al.¹⁰ (Table 1).

The catalytic center in our calculations consists of Pd(II) coordinated by $\text{H}_2\text{PCH}=\text{CHPH}_2$ (Chart 1b), which is used to model the chiral Me-DUPHOS (Chart 1a) ligand of the original study by Sen.³ We have chosen $\text{H}_2\text{PCH}=\text{CHPH}_2$ as a model since it preserves all of the features which the Me-DUPHOS ligand imparts on the reaction, except the ability to induce chirality in the growing chain. We shall consider enantioselective polymerization in a later study.

[†] Email: pmargl@zinc.chem.ucalgary.ca.

[‡] Email: ziegler@zinc.chem.ucalgary.ca.

[®] Abstract published in *Advance ACS Abstracts*, November 15, 1996.

(1) Margl, P. M.; Ziegler, T. *J. Am. Chem. Soc.* **1996**, *118*, 7337.

(2) Sen, A.; Jiang, Z. *Macromolecules* **1993**, *26*, 9111.

(3) Jiang, Z.; Sen, A. *J. Am. Chem. Soc.* **1995**, *117*, 4455.

(4) Lain, T.-W.; Sen, A. *Organometallics* **1984**, *3*, 866.

(5) Drent, E.; Broekhoven, J. A. M. v.; Doyle, M. J. *J. Organomet. Chem.* **1991**, *417*, 235.

(6) Valli, V. L. K.; Alper, H. *J. Polym. Sci., Part A: Polym. Chem.* **1995**, *33*, 1715.

(7) Kacker, S.; Sen, A. *J. Am. Chem. Soc.* **1995**, *117*, 10591.

(8) Sen, A. *Acc. Chem. Res.* **1993**, *26*, 303.

(9) Lai, T.-W.; Sen, A. *Organometallics* **1984**, *3*, 866.

(10) Rix, F. C.; Brookhart, M.; White, P. S. *J. Am. Chem. Soc.* **1996**, *118*, 4746.

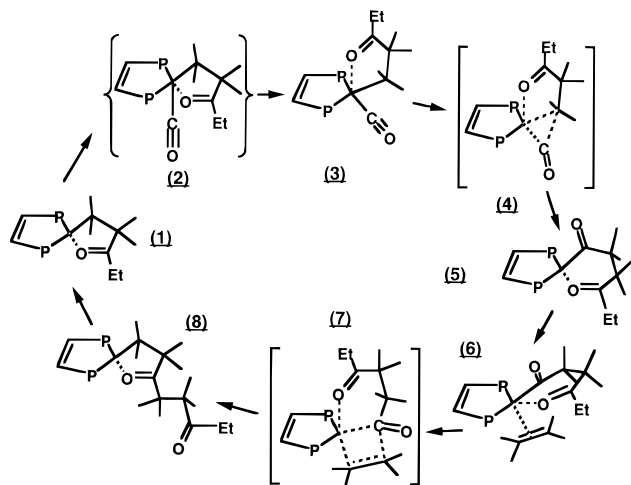


Figure 1. Flow chart of the productive section of the catalytic cycle leading to an alternating CO/olefin copolymer. Stages of the reaction are identified with numbers. Species in square brackets refer to transition states. Structures in curved brackets refer to unstable (not observable) species. All species referred to in this work carry a single positive charge.

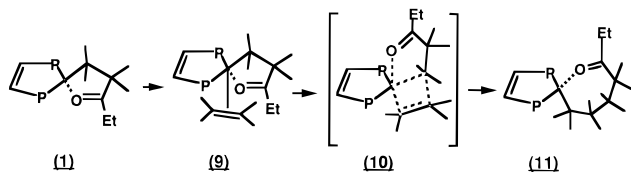


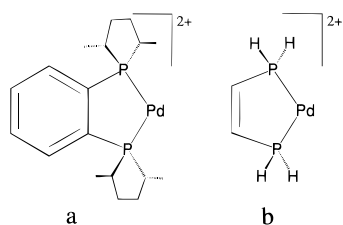
Figure 2. Misinsertion of olefin during the catalytic copolymerization of CO and olefin (see also Figure 1).

Table 1. Activation Energies, as Derived by ADF, Compared to the Experimentally Derived Values found by Rix et al.^{10 a}

reaction step	ΔH^\ddagger (ADF)	ΔG^\ddagger (Rix et al.)	deviation
$\text{LPd}(\text{C}_2\text{H}_4)(\text{Et})^+ \rightarrow \text{LPd}(\text{Bu})^+$	+65 ^b	+81.2 (-25 °C)	-16.2
$\text{LPd}(\text{R})(\text{CO})^+ \rightarrow \text{LPd}(\text{Ac})^+$	+48 ^b	+64.4 (-66 °C)	-16.4
$\text{LPd}(\text{Ac})(\text{C}_2\text{H}_4)^+ \rightarrow \mathbf{1}$	+58 ^b	+69.5 (-46 °C)	-11.5
$\mathbf{3a} \rightarrow \mathbf{5a}$	+49	+62.3 (-66 °C)	-13.8
$\mathbf{6} \rightarrow \mathbf{8}$	+64	+72.0 (-44 °C)	-8.0

^a All values are in kJ/mol. Rix et al. used phenanthroline as a bidentate ligand, whereas for the ADF calculations, $\text{PH}_2\text{CHCHPH}_2$ was used. ^b Taken from Margl and Ziegler.¹

Chart 1



Computational Details

Stationary points on the potential energy surface were calculated with the program ADF, developed by Baerends et al.,^{11,12} and vectorized with the methods by Ravenek.¹³ The

(11) Baerends, E. J. Ph.D. Thesis, Free University, Amsterdam, The Netherlands, 1973.

(12) Baerends, E. J.; Ellis, D. E.; Ros, P. *Chem. Phys.* **1973**, *2*, 41.

(13) Ravenek, W. In *Algorithms and Applications on Vector and Parallel Computers*; te Riele, H. J. J., Dekker, T. J., van de Horst, H. A., Eds.; Elsevier: Amsterdam, The Netherlands, 1987.

numerical integration scheme applied for the calculations was developed by te Velde et al.^{14,15} The geometry optimization procedure was based on the method due to Versluis and Ziegler.¹⁶ The electronic configurations of the molecular systems were described by a triple- ζ basis set on palladium^{17,18} for 4s, 4p, 4d, 5s, and 5p. Double- ζ Slater-type orbital (STO) basis sets were used for carbon (2s, 2p), hydrogen (1s), phosphorus (3s, 3p), and oxygen (2s, 2p) that were augmented with a single 3d polarization function except for hydrogen where a 2p function was used. The $1s^2 2s^2 2p^6 3s^2 3d^{10}$ configuration on palladium, the $1s^2$ shell on carbon and oxygen as well as the $1s^2 2s^2 2p^6$ shells on phosphorus were assigned to the core and treated within the frozen-core approximation. A set of auxiliary¹⁹ s, p, d, f, and g STO functions, centered on all nuclei, was used in order to fit the molecular density and to represent Coulomb and exchange potentials accurately in each self-consistent field (SCF) cycle. Energy differences were calculated by including the local exchange-correlation potential by Vosko²⁰ et al. with Becke's²¹ nonlocal exchange corrections and Perdew's^{22,23} nonlocal correlation correction. Geometries were optimized, including nonlocal corrections. First-order scalar relativistic corrections²⁴⁻²⁶ were added to the total energy, since a perturbative relativistic approach is sufficient for 4d metals. Since all of the systems investigated in this work show a large HOMO-LUMO gap of at least 2 eV, a spin-restricted formalism was used for all calculations. No symmetry constraints were used, except where explicitly indicated. Saddle-point determinations were done by a linear transit search from reactant to product along an assumed reaction coordinate. In each step along the reaction coordinate, all other degrees of freedom were optimized. A fine linear transit grid of 0.01 Å was used around the saddle point. Due to the large number of slow vibrations, no transition state search based on the second derivatives of the total energy could be carried out.

Results and Discussion

The Productive Cycle. In a previous study,¹ the energetics of the processes leading from PdPPH^+ to compound **1** have been described. To form a strictly alternating copolymer, species **1** must take up a CO molecule and insert it into the chain (Figure 1). A geometry optimization of a tentative five-coordinate CO complex with the CO molecule in the apical position directly yielded species **3a**, with the CO molecule rotated into the equatorial plane and the chelating carbonyl group now occupying the apical position. The total energy of **3a** lies 32 kJ/mol below that of **1**. This is in good agreement with an exothermicity of $\Delta G^{298} = -10$

(14) te Velde, G.; Baerends, E. J. *J. Comput. Chem.* **1992**, *99*, 84.

(15) Boerrigter, P. M.; te Velde, G.; Baerends, E. J. *Int. J. Quantum Chem.* **1988**, *33*, 87.

(16) Versluis, L.; Ziegler, T. *J. Chem. Phys.* **1988**, *88*, 322.

(17) Snijders, J. G.; Baerends, E. J.; Vernoijs, P. *At. Nucl. Data Tables* **1982**, *26*, 483.

(18) Vernoijs, P.; Snijders, J. G.; Baerends, E. J. *Slater Type Basis Functions for the Whole Periodic System*; Internal report (in Dutch); Department of Theoretical Chemistry, Free University: Amsterdam, The Netherlands, 1981.

(19) Krijn, J.; Baerends, E. J. *Fit Functions in the HFS Method*; Internal Report (in Dutch); Department of Theoretical Chemistry, Free University: Amsterdam, The Netherlands, 1984.

(20) Vosko, S. H.; Wilk, L.; Nusair, M. *Can. J. Phys.* **1980**, *58*, 1200.

(21) Becke, A. *Phys. Rev. A* **1988**, *38*, 3098.

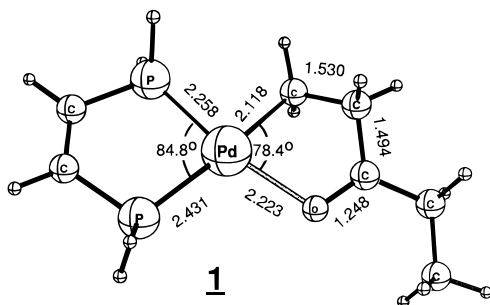
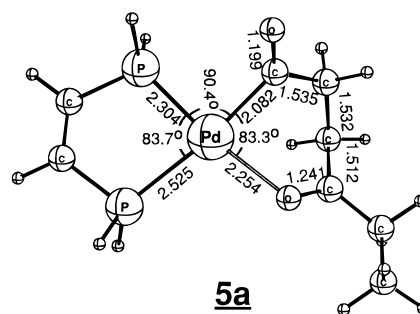
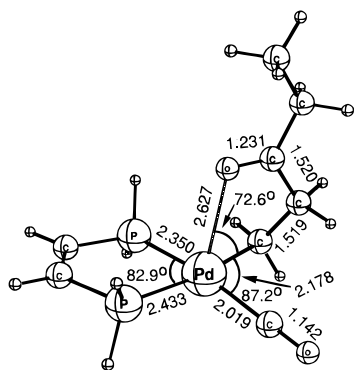
(22) Perdew, J. P. *Phys. Rev. B* **1986**, *34*, 7406.

(23) Perdew, J. P. *Phys. Rev. B* **1986**, *33*, 8822.

(24) Ziegler, T.; Tschinke, V.; Baerends, E. J.; Snijders, J. G.; Ravenek, W. *J. Phys. Chem.* **1989**, *93*, 3050.

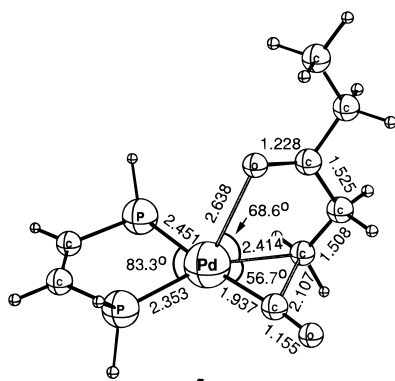
(25) Snijders, J. G.; Baerends, E. J. *Mol. Phys.* **1978**, *36*, 1789.

(26) Snijders, J. G.; Baerends, E. J.; Ros, P. *Mol. Phys.* **1979**, *38*, 1909.

**1****5a****3a**

kJ/mol (recalculated from K_6/K_3 in ref 10) as derived by Rix et al.,¹⁰ considering that this contains a considerable positive entropic contribution which is not contained in our result. From a calculation where we remove the chelating bond from the Pd center by rotating the chain (**3b**), we determine the strength of the chelating bond as 29 kJ/mol, which is much weaker than the 104 kJ/mol determined for an in-plane chelating bond in **1**.¹ The weaker bond between Pd and O is also expressed by the much longer chelate bond distance in **3a** as compared to **1**.

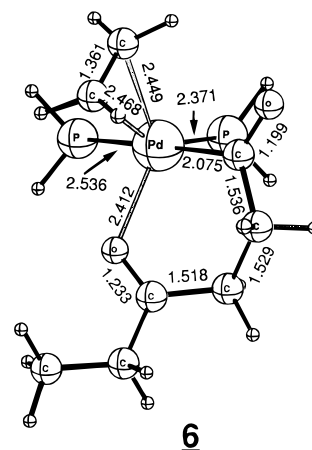
A transition state for the insertion of CO into the Pd–C $_{\alpha}$ bond was located at a C $_{CO}$ –C $_{\alpha}$ distance of 2.107 Å, which is slightly longer than the 2.060 Å that was previously found¹ for the insertion of CO into the Pd–ethyl bond. The transition state **4** lies 49 kJ/mol above **3a** (Rix et al.: $\Delta G^{\ddagger} = 62.3$ kJ/mol at -66 °C,¹⁰ Table 1), which coincides well with the 48 kJ/mol activation barrier obtained¹ for the insertion of CO into the Pd–ethyl bond. The chelating bond persists throughout the

**4**

transition state. As the transition state decays into the insertion product **5a**, the chelating bond returns from the axial position to the preferred equatorial one. The equatorial chelating bond has a strength of 51 kJ/mol,

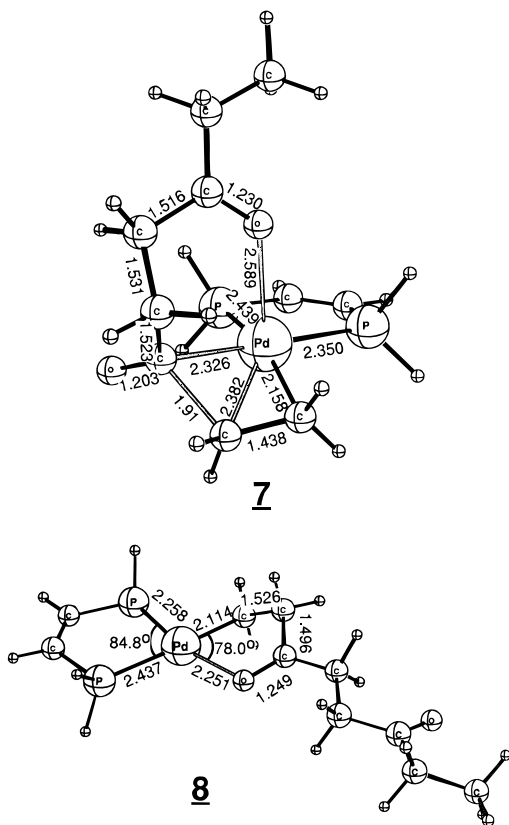
as determined by removing the chelate oxygen from the metal and the coordination plane (**5b**). Therefore, the chelating bond of **5a** is not nearly as strong as the chelating bond of **1**, but the chelate bond strength suffices to turn the reaction decidedly exothermic. In contrast to this, the insertion of CO into a Pd–ethyl bond is only exothermic by -12 kJ/mol, even though the product is stabilized by 31 kJ/mol due to the formation of a dihapto-carbonyl.¹

Since at this stage insertion of a CO unit into the chain has already been ruled out on a thermodynamic basis,¹ the only avenue left open to the system is to insert a C $_2$ H $_4$ unit. Uptake of C $_2$ H $_4$ starting from an apical position yields structure **6** by geometry optimization. The existence of a purely equatorially coordinated

**6**

C $_2$ H $_4$ has been checked, but geometry optimization invariably led to the trigonal bipyramidal species **6**, with C $_2$ H $_4$ occupying an equatorial position of the trigonal bipyramid. C $_2$ H $_4$ uptake has a modest exothermicity of -25 kJ/mol, as expected in a case where the olefin must partially displace a strong chelating bond. This is in excellent agreement with a value of $\Delta H^{\ddagger} = -27.2$ kJ/mol found by experiment in CD $_2$ Cl $_2$ solution.¹⁰

The transition state for olefin insertion, **7**, lies 64 kJ/mol above **6**, which coincides well with the value of $+58$ kJ/mol derived previously for the insertion of C $_2$ H $_4$ into a Pd–COC $_2$ H $_5$ bond.¹ Rix et al. determined a ΔG^{\ddagger} of $+72$ kJ/mol for the reaction **6** \rightarrow **8** in CD $_2$ Cl $_2$ at -44.4 °C. In the transition state geometry, the C $_{CO}$ –C $_{olefin}$ bond is 1.91 Å long, as compared to 1.858 Å in the transition state for insertion of olefin into the Pd–COC $_2$ H $_5$ bond.¹ The transition state is stabilized by a chelating bond from the apical position of an approximate square pyramid. The insertion reaction is exothermic by -48 kJ/mol, which is considerably (26 kJ/mol) less than the value of -74 kJ/mol for the insertion of olefin into the Pd–COC $_2$ H $_5$ bond.¹ We have shown that the stabiliza-



tion from an apical chelating bond is -29 kJ/mol for **3a**, and thus the difference of 26 kJ/mol is not surprising since the apical chelating bond is removed when going from **7** to **8**. The product state **8**, similar to the initial state **1**, has only one strongly stabilizing chelating bond, and thus it can be stated that **1** serves as an accurate model for the resting state of the alternating copolymerization.

The reaction of **1** \rightarrow **8** represents the insertion of one CO/C₂H₄ unit from the resting state **1** to the equivalent resting state **8**. Thus, the corresponding heat of reaction calculated as -137 kJ/mol (Figure 3) should be a good estimate for the polymerization enthalpy of one CO/C₂H₄ unit in polyketones. This number is short of the 200 kJ/mol gained by incorporating two ethylene units into a polyolefin,¹ thus confirming that CO/C₂H₄ copolymerization is thermodynamically less favorable than pure ethylene polymerization. We shall now turn to the kinetic factors favoring CO/C₂H₄ copolymerization over pure ethylene polymerization by comparing the barrier of CO insertion into the metal-alkyl bond (**3a** \rightarrow **5a**) with the alternative misinsertion of ethylene into the same bond (Figure 2).

C₂H₄ Misinsertion into an Ethylene-Terminated Polyketone Chain. We started our study of the misinsertion by investigating whether an adduct where the C₂H₄ molecule is bound to the apical site of **1** is stable. A geometry optimization of species **9** shows that at the nonrelativistic level, the ethylene is weakly bound to **1**, with an adduct formation energy of only -2 kJ/mol. The addition of the first-order relativistic perturbation corrections renders the adduct formation to be endothermic by 1 kJ/mol (Figure 4). This means that ethylene has in fact no sticking probability at the metal complex, which drastically reduces its ability to further insert into the copolymer. No evidence for an ethylene bound in the equatorial position was found; geometry

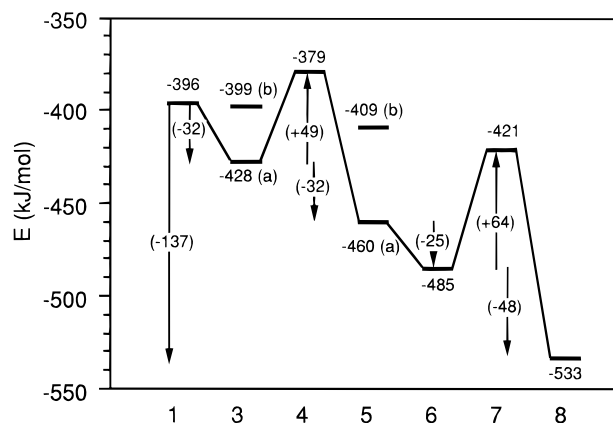


Figure 3. Energy profile for the productive part of the catalytic copolymerization of CO and C₂H₄. Energies in kJ/mol. Stages of the reaction are identified with numbers (see Figure 1); energies of free monomers are included. Different isomers of a given species are distinguished with alpha-numerics. For easy compatibility, energies are given with respect to the species PdPPH⁺ (see Margl and Ziegler¹) and that of the free monomers.

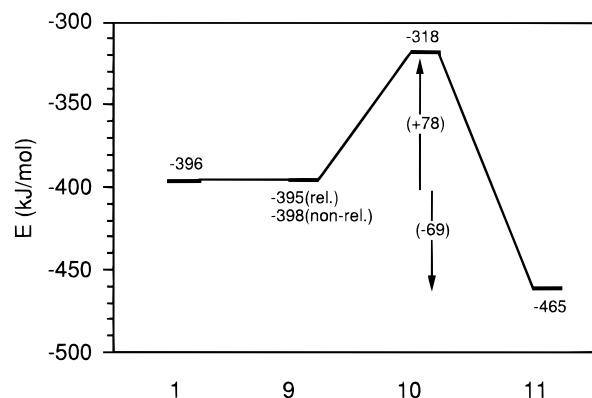
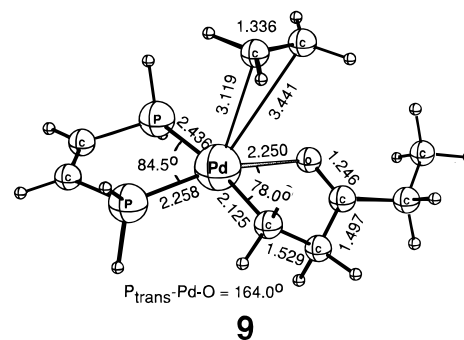
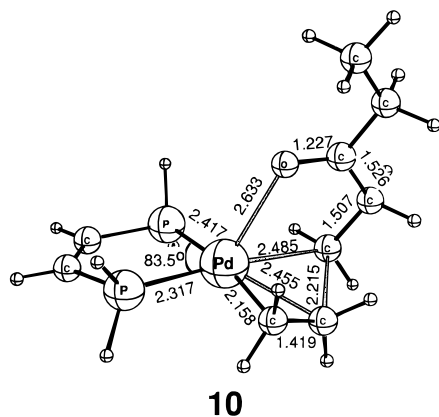


Figure 4. Energy profile for the C₂H₄ double insertion. Units and conventions as in Figures 1 and 3.

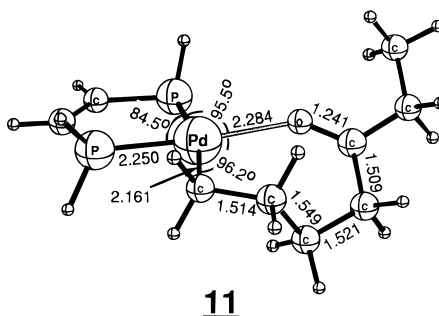


optimization of a tentative species with equatorial ethylene coordination invariably led back to **9**. Furthermore, the ethylene molecule must partially displace the strong chelating bond of **1** in order to be able to insert into the Pd-C₂H₄COC₂H₅ bond. In contrast to our findings, Rix et al. found the reaction of **1** with C₂H₄ to be exothermic ($\Delta H^{\circ} = -32.6$ kJ/mol). From the viewpoint of our calculations, this discrepancy is difficult to explain, especially since the results of Rix et al. for the complexation of C₂H₄ by **5a** ($\Delta H^{\circ} = -27.2$ kJ/mol) coincide very well with ours ($\Delta H = -25$ kJ/mol). Furthermore, our calculations indicate that the chelating bond in **1** (-104 kJ/mol) is much stronger than the chelate bond of **5a** (-51 kJ/mol), so that it seems

reasonable to expect that ethylene uptake for **1** should be much less exothermic than for **5a**. One might argue that the solvent (CD_2Cl_2) which was used in the experiments might somehow disrupt the chelation effect and enhance olefin binding to **1**. However, in the absence of detailed solvation data for the complexes in question, our reasoning must remain merely speculative. Insertion is achieved via a transition state **10** which lies 78 kJ/mol above **9**. This is much higher than any barrier



encountered in the cycle from **1** to **8**, so that we can now firmly state that multiple olefin insertion is kinetically unfavorable compared to $\text{CO}/\text{C}_2\text{H}_4$ insertion. Chances of insertion are also greatly lessened by a zero-sticking probability of the incoming ethylene. However, the thermodynamic driving force for the formation of **11** is higher in this case (-69 kJ/mol) than it is for uptake and insertion of CO (**1** \rightarrow **5a**: -64 kJ/mol), which would be the competing step in the productive cycle. Our



activation barrier of 78 kJ/mol is in good agreement with a value of 81.2 kJ/mol obtained for insertion of ethylene into a Pd-ethyl bond by Rix et al.¹⁰ The corresponding activation energy for the insertion of ethylene into the Pd-ethyl bond obtained in our previous study was +65 kJ/mol.¹

Conclusion

We have studied the Pd(II)-assisted homogeneous catalytic copolymerization of olefin and carbon monoxide, **1** \rightarrow **8**. The catalytic center in our calculations consisted of Pd(II) coordinated by $\text{H}_2\text{PCH}=\text{CHPH}_2$ (Chart 1b), which is used to model the chiral MeDUPHOS (Chart 1a) ligand of the original study by Jiang and Sen.³ Throughout the process, the growing chain was allowed to coordinate to the metal center through a carbonyl group. The $\text{CO}/\text{C}_2\text{H}_4$ copolymerization consists of insertion of CO into a metal-alkyl bond followed by insertion of ethylene into a metal-acyl bond. The first process has an internal barrier of 49 kJ/mol and a reaction enthalpy of -64 kJ/mol. The activation barrier for the second process is 64 kJ/mol with a heat of reaction of -73 kJ/mol. Also considered was the misinsertion of ethylene into the metal-alkyl bond. This process is kinetically less favorable than CO insertion due to the lack of a thermodynamically stable ethylene π -complex and the high barrier ($+78$ kJ/mol) associated with insertion of ethylene into the Pd- C_2H_4 -CO-R bond. It is concluded that $\text{CO}/\text{C}_2\text{H}_4$ copolymerization is thermodynamically less favorable than that of pure olefin polymerization. However, the lower barrier of insertion for CO compared to ethylene into the metal-alkyl bond makes $\text{CO}/\text{C}_2\text{H}_4$ copolymerization the kinetically more feasible process. Furthermore, in combination with the recently published data of Rix et al.,¹⁰ our studies afford a unique opportunity to validate the nonlocal DFT approach with respect to experimental results. Although their data¹⁰ is derived from a N-based (phenanthroline) system, as opposed to the P-based system used in our work, excellent agreement is obtained between the experimental and theoretical barrier heights, with an average deviation of -13.2 kJ/mol (-3 kcal/mol) between the experimental and nonlocal DFT results. Although we compare ΔH^\ddagger to ΔG^\ddagger values, for transition states such as those studied, the entropic contributions should be fairly small¹⁰ since they represent unimolecular reactions.

Acknowledgment. This work has been supported by the National Sciences and Engineering Research Council of Canada (NSERC) as well as by the donors of the Petroleum Research Fund, administered by the American Chemical Society (ACS-PRF No. 31205-AC3). P.M. thanks the Austrian Fonds zur Förderung der wissenschaftlichen Forschung (FWF) for financial support within project JO1099-CHE. T.Z. thanks the Canada Council for a Killam professorship.

OM960521O